

# 591. Diagnostics procedure for identification of rubs in rotor bearings

V. Barzdaitis<sup>1</sup>, M. Bogdevičius<sup>2</sup>, R. Didžiokas<sup>3</sup>

Kaunas University of Technology, A. Mickevičiaus St. 37-120, LT44244, Kaunas, Lithuania  
vytautas.barzdaitis@ktu.lt

Vilnius Gediminas Technical University, Plytinės St. 27, LT10105, Vilnius, Lithuania  
marijonas.bogdevicius@vgtu.lt

Klaipėda University, MMI, Bijūnų St. 17, LT91225, Klaipėda, Lithuania  
rimantas.didziokas@ku.lt

(Received 25 September 2010; accepted 9 December 2010)

**Abstract:** it is well known that old design high-power generating machines were on duty for more than 35-40 years and will successfully continue operation after proper renovations and overhauls. this paper considers vibrational characteristics of the old continuously operated 110 mw turbounit with steam turbines and electric generator rotating system running at nominal speed of 3000 rpm. vibration and technological parameters were systematically monitored in the course of 5 years after installation of condition monitoring and diagnostics system, which is based on measurements of rotor relative vibration displacement. it is demonstrated that application of optimized vibration monitoring and diagnostic system and several vibration data formats is effective in evaluation of overhaul quality through vibration severity of rotor system and identification of causes of these vibrations. the research focus in the reported research work is placed on inspection of mechanical effect of horizontal rotor-to-stator rubbing in upper part of journal bearing. the validity of the results is verified during overhauls and renovations, and can reduce the possibility of bearing failures.

**Keywords:** turbounit, journal bearings vibration, diagnostics, rotor-to-stator rubs

## Nomenclature

$\{B\}$	right hand vector	$[N_w]$	matrix of shape functions
$[C]$	damping matrix	NE	total number of finite element
c	mean radial clearance	$\{P\}$	vector of nodal pressure
e	eccentricity	p	pressure of liquid
$[G]$	gyroscopic matrix	$p_a$	ambient pressure
$[H]$	matrix of total system of equations	$R_B$	radius of journal bearing
h	film thickness	$R_R$	radius of journal
$\{F\}$	load vector of rotor	Re	Reynolds number
$[J]$	Jacobi matrix	s	circumferential coordinate
$[K]$	stiffness matrix of rotor	x	longitudinal axe of journal bearing
$k_x, k_s$	circumferential turbulence coefficients	$U_x, U_s$	velocity components
$[M]$	mass matrix	V	volume of defects
$[N_v]$	matrix of shape functions	v	displacement of journal in the Y direction

$w$	displacement of journal in the Y direction	$\{\ddot{q}\}$	vector of nodal accelerations
$\mu$	liquid viscosity	$\psi$	attitude angle
$\varphi_R$	journal angle	Subscripts	
$\varphi_B$	bearing angle	<b>B</b>	bearing
$\dot{\varphi}_R$	journal angular velocity	<b>def</b>	defects
$\theta$	circumferential coordinate	<b>R</b>	journal
$\{q\}$	vector of nodal displacements	<b>v</b>	displacement in the Y direction
$\{\dot{q}\}$	vector of nodal velocities	<b>w</b>	displacement in the Z direction

## Introduction

Rotating machinery is dominated in power generation industry. Stationary technical condition monitoring, protection and diagnostic systems (MDS) of the machinery, which are installed not only in new critical machines, but in old design high power generating machines during renovation processes, improve machine efficiency. Vibration data bases and data formats mostly are simple and contain limited information for a diagnostician in old design machines in comparison with possibilities of modern MDS. Rotor relative vibration displacement measurement with contactless proximity probes is a new area in diagnostics [1]. In turbounits higher efficiency is achieved by tightening operating clearances between elements, including journal bearings. Reduced clearances lead to stator-to-rotor rubs. If rotor misalignment is significant, despite that most common types of rubs are blade tip and seal rubs [2], the bearings rubs are dominated. These rubs are known as full annular rubs and partial rubs. The partial rub – when the rotor maintains contact with the bearing part only during the small portion of the rotor cycle is encountered more frequently in comparison with full annular rubs. The repetitive contact rotor with the stator causes more significant impacting and severe vibrations during rubbing. After the rub (impact) the rotor orbiting is characterized by the free lateral vibration with frequency equal to one or combination of rotor natural frequencies. Most probably it is the lowest natural frequency in the lateral mode. But from the diagnostic practice point of view it is not only difficult to identify location of rubbing phenomenon in operating turbounit, but it is impossible to determine causalities of rubs. This is a crucial problem for old design turbounits with prolonged continuous operation without modern MDS. The main solution is to replace bearing housings, absolute vibration measurements performed with seismic transducers that are acceptable for monitoring of rotors with rolling element bearings by the relative or absolute vibration displacement measurements of the rotors with proximity probes [3, 4]. Early experiences on steam turbines and generators were restricted to the measurement of bearings housings absolute vibration using only seismic transducers [5]. As diagnostics practice revealed the journal bearing housings vibration measurements with seismic transducers can serve to identify approximately the rubbing start moment, but not exact location of this event. Theoretical modeling and experimental research frequently are conducted with laboratory equipment and tested with machines in situ [7]. But to install modern MDS in old design rotors, especially to locate proximity probes inside the bearings or as near as possible at the bearings, sometimes is challenging and depends on rotor design. The rotors with relative vibration displacement measurement of journal bearings are essential for proper diagnostics of many malfunctions and especially of the rubbing. This paper reports new research data concerned with evaluation of the overhauls and changes in machine dynamics between two overhauls of high power turbines rotating system with rubbing in journal bearings. Turbounit rotating system condition monitoring and diagnostics was accomplished by means of newly installed MDS. The objective is improvement of accuracy of diagnostics of high power old design turbounit, more

precise evaluation of vibration severity and identification of rubbing causes in the upper part of the bearing.

## Diagnostics approach and testing methodology

### Object of research

The rotating system of 110 MW power turbounit and 3000 rpm rotation speed with three steam turbines, electric generator, and exciter and equipped with new stationary condition monitoring and diagnostic system BNC 3500 (USA) illustrated in Fig. 1. The modern MDS was installed after 25 years of the continuous operation of the machine. Primary stationary condition monitoring system was based only on bearings housings absolute vibration velocities measurements  $v_{rms}$  values without diagnostics. Vibration displacement measurements of the rotors relative to the bearings had not been performed earlier.

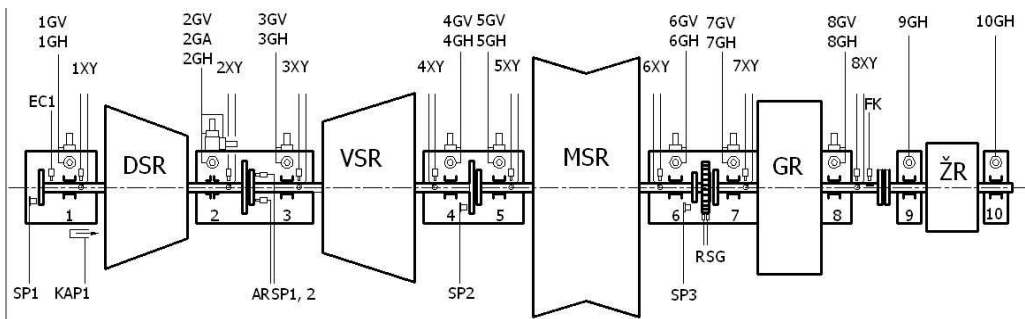


**Fig. 1.** Turbounit scheme: high DSR, middle VSR and low MSR pressure steam turbine rotors, generator and exciter rotors (GR, ŽR); 1, 3-10 journal bearings, 2-thrust tilting pad bearing; 1XY,...,8XY-non-contacting sensors; EC1, SP1,..., SP3, ARSP1,2, KAP1 - displacement transducers; RSG - rotation speed sensors; FK - Keyphasor; 1GV, 2GA,...,10GH - seismic transducers (V vertical, H horizontal and A axial)

### Diagnostics methodology

Turbounit vibration measurements and analysis of the results were carried out before and after two overhauls and conducted periodically during continuous 5-year operation term until to now. The rotors relative vibration displacement measurements were provided close as possible to the all eight bearings. Most frequently occurring breakdowns in high- power turbounit rotor systems are journal bearing failures during run-up and coast-down. These damages caused by uneven thermal deformations of massive cases and less massive rotors at run-up, bent rotors, unbalance of the rotors, high vibration levels during coast-down at resonances, lateral or/and angular misalignment between rotors and couplings, oil or steam induced whip/whirl self-excited vibration, etc. If rotor-to-stator rubbing occurs the vibrations may become excessive and may cause a serious damage to rotor elements or lead to catastrophic sudden failure of the machine. The proximity probes as non-contacting sensors measured shaft dynamic motion – vibration displacement peak-to-peak magnitude  $s_{p-p}$  (AC signal) and shaft position in the bearing (gap) relative to the probe mounting location (DC signal). The vibration magnitude  $S_{(p-p)\max} = 2s_{\max}$  is the higher value of the peak-to-peak displacement measured in two selected orthogonal measurement directions. The measured values are interpreted in main vibration data formats that are effective in diagnostics and identification of the rubs in journal bearings and allow determination of casualties of rubbing phenomenon. Because there are

considerable inconsistencies between bearing housings absolute vibration and shafts relative vibration values the diagnostics was based on measurements of rotor relative vibration displacements and analysis of results [6].

**Long-term diagnostics results**

The condition monitoring and diagnostics of turbounit was performed continuously between two overhauls and temporal variation of relative vibration displacements of eight bearing shafts during operation at maximum loading is presented in Fig.2. Vibration displacements monitoring results indicate that low pressure rotor MSR 5<sup>th</sup> bearing had severe vibration displacement values since the first overhaul up to the second.

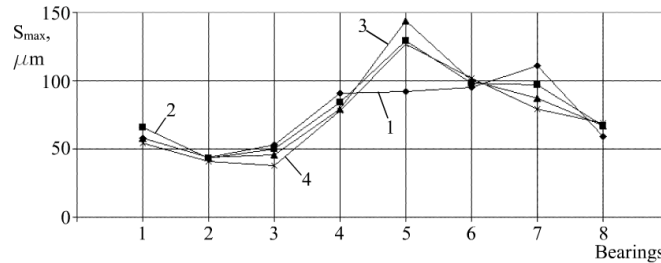


**Fig. 2.** Maximum values of relative vibration displacements  $s_{max}$  of the rotor bearing shafts under maximum loading at continuous operation: 1 – 2005 (after first overhaul), 98 MW; 2 – 2007, 99 MW; 3 – 2008; 106 MW and 4 – 2009 (before second overhaul), 102 MW

Fig. 3 reveals that the most sensitive to the loading from the vibration intensity point of view are DSR 2<sup>nd</sup> and VSR 3<sup>rd</sup> bearings when loading varies from maximum value 102 MW up to free run (FR) when tested before scheduled second overhaul (2009). The 2<sup>nd</sup> and 3<sup>rd</sup> bearing vibration values indicate significant changes in vibration displacement amplitudes and in phases.

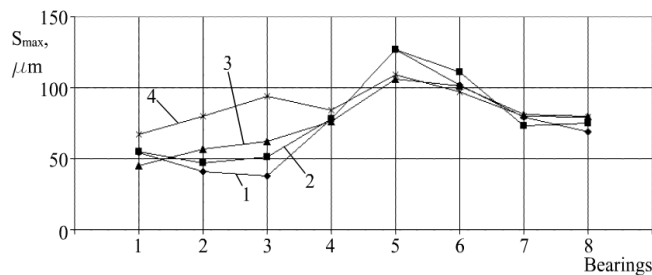


**Fig. 3.** Maximum values of relative vibration displacement  $s_{max}$  ( $2 s_{max} \approx s_{p-pmax}$ ) of the eight bearing shafts measured before 2009 scheduled major overhaul at varying loading from 102 MW up to FR: 1 – 2009 03 20, 102 MW; 2 – 2009 04 15, 86 MW; 3- 29 MW and 4 - 2009 04 16, FR

**Rubbing of rotor against a stationary part**

Rub is a dangerous contact between a rotating and stationary part and leads to direct damage to the contacting parts. Rub is the secondary effect that is caused by some other malfunction, which produces a combination of average and dynamic shaft centerline position that exceeds the available clearance between the rotor and the stator. The average shaft centerline plot (ASCP) indicates changes in the average position of the shaft centerline in two dimensions and is constructed from the DC part of the vibration signals. The extreme ASCP

(static) can be caused by excessive radial loads, looseness and external or internal misalignment caused by a warped casing, steam piping strain, foundation deformations and looseness, uneven thermal growth or out of position by internal parts.

Extreme dynamic shaft position can be induced by high vibrations, due to excessive unbalance, rotor bow, or instability (rub, oil-steam-fluid-induced instability, resonance). When the rotor moves away from the bearing, the spring stiffness of the rotor will decrease, producing a change (increase) in vibration response. Rub produces simultaneous, nonlinear changes in both the force and the dynamic stiffness. The rubbing forces (radial and tangential friction) suddenly appear and disappear: the radial force acts in the direction of the rotor center to strongly accelerate the rotor away from the contact point; the tangential friction force appears which is proportional to the instantaneous magnitude of the radial force and the coefficient of friction at the sliding interface. The tangential friction force acts opposite to the surface velocity of the shaft. It produces a torque on the rotor and, at the same time, tries to accelerate the rotor centerline in the reverse precession direction. For this reason, partial radial rub produces reverse components in the full spectrum. A side effect of the tangential friction force is that it acts as an agent to transfer the kinetic energy of rotation to radial vibration energy [1]. This process produces a self-excited vibrations that are larger in amplitude than would be possible without the energy transfer. Partial radial rub produce a self-excited, large amplitude, subsynchronous vibration at subharmonics ( $1/2X$ ,  $1/3X$ ,  $1/4X$ , etc.) frequencies. This self-excited vibration is always associated with a modified natural frequency of the rotor system. During the experimental testing of the turbounit the main vibration data formats were designed to identify the rubbing event.

Like most malfunctions, diagnosis of rub involves correlation of different types of vibration and data of technological parameters. It is important to correlate the steady state and transient vibration data formats: average shaft centerline plots (ASCP), direct orbit and time base plots; full spectrum, including cascade and waterfall plots,  $1X$  Bode and polar plots, vibration signal trends. The result of rub effects is a complex rotor dynamic response that produces a wide variety of symptoms.

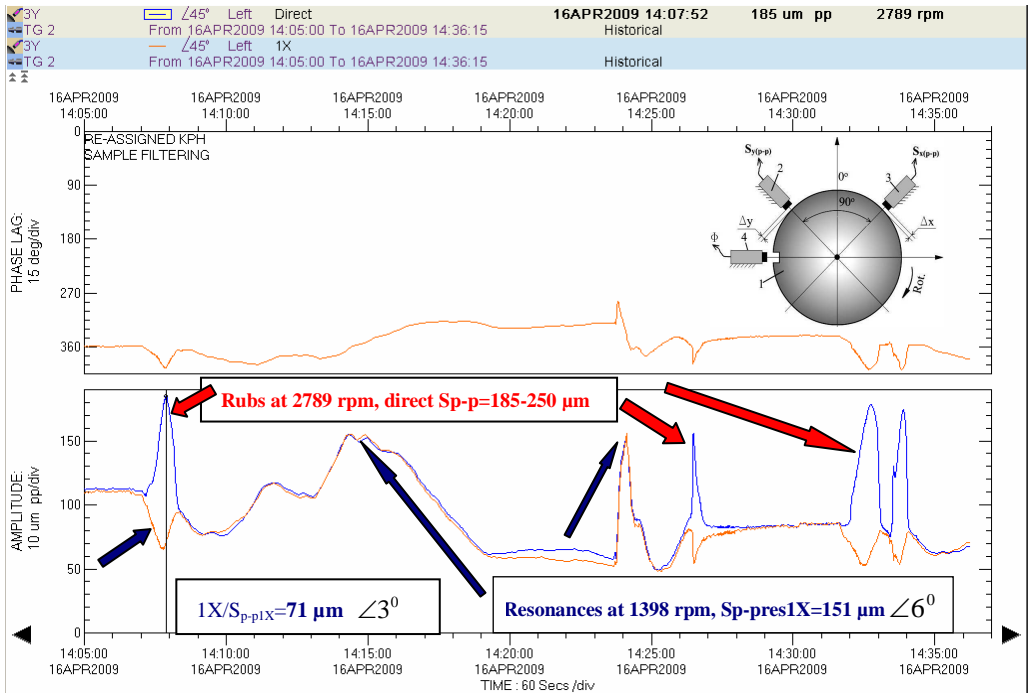
**Trend plot** The trend plot of vibration displacement magnitude and phase presented in Fig. 4 and acquired at repeated shutdowns and run-ups modes. The severe vibrations occurred at rotation speeds  $\sim 2750$ - $2900$  rpm and rotor system first natural frequency measured as  $1390$ - $1341$  rpm. The experimental testing revealed that sudden increase in direct vibration displacement amplitude occurred at  $\sim 2789$  rpm as indicated in Fig. 4. The rotor system has a natural frequency at a subharmonic ( $\sim 1398$  rpm) of the rotor operating speed (at  $\sim 2789$  rpm), than, after one cycle of this subsynchronous free vibration  $1/2X$ , the rub impulse will recur. Rotation speed  $2789$  rpm (synchronous  $1X=46.48$  Hz frequency) vibration played a role by increasing the lateral velocity of the rotor at the moment of contact. The experimental testing verified that the rub induced instability in the bearing occurred at run-up (with steam) and at shutdown (without steam).

### **ASCP – average shaft centerline plot**

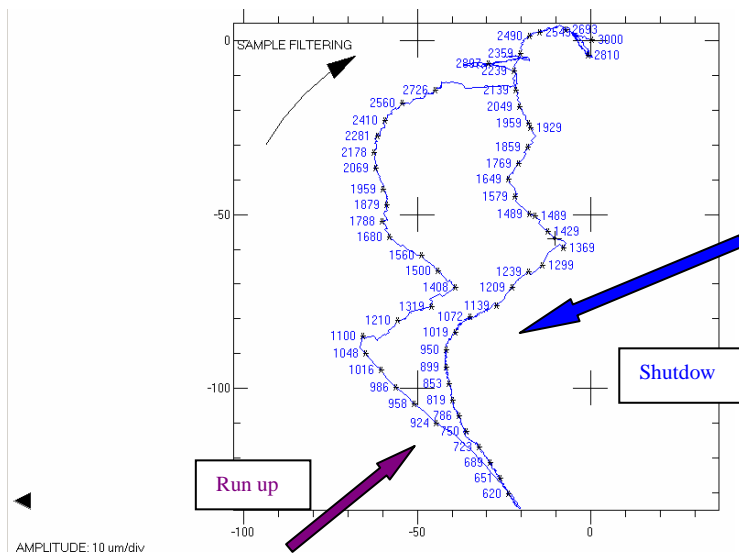
The ASCP indicates changes in the average position of the shaft centerline in two dimensions and is constructed from the DC signals of the two sensors. The ASCP of the middle pressure rotor with damaged (Fig. 5) and new (Fig. 6) 3<sup>rd</sup> bearing accentuated the initial information in evaluation of changes occurred in the bearing during 5 years exploitation after first overhaul. The 3<sup>rd</sup> bearing's shaft abnormal shift centerline position registered just after overhaul at 2005 as shown in Fig. 6 (left). The normal ASCP for hydrodynamic fluid film bearing measured after overhaul at 2009 as illustrated in Fig. 6 (right). The ASCP data format served as initial indicator for prediction of the inevitable damage that will take place in the 3<sup>rd</sup>

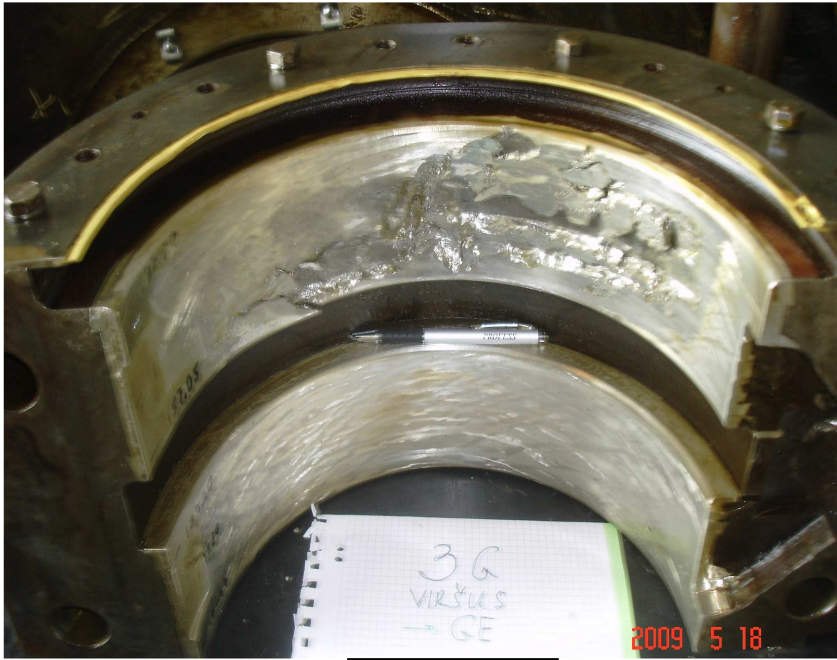
bearing in the future. The inaccessible large misalignment between DSR and VSR rotors was made during first overhaul of machine at 2005 that caused rubbing in the bearing, Fig. 5.

The ASCP reveals a dramatic shift centerline position at shutdown from 3000 rpm up to 2900 rpm (without rub), from 2900 rpm up to ~2758 (rubbing, Fig. 4) and from ~2750 rpm up to 2469 rpm (without rub), Fig. 7. The centerline behavior is abnormal at run-up as at shutdown mode for fluid film 3<sup>rd</sup> bearing.



**Fig. 4.** 3<sup>rd</sup> bearing's shaft relative vibration displacement  $s_{p-p}$  and phase trend plots at shutdowns (rubblings at ~2789 rpm direct  $s_{p-p}$ =185-250  $\mu\text{m}$ ; 1X=46,48 Hz frequency vibration amplitude  $s_{p-p}$ =71 $\mu\text{m}$ ; at resonance 1398 rpm  $s_{p-pres}$ =140-151 $\mu\text{m}$ )





Damaged bearing

Fig. 5. Abnormal ASCP of the damaged 3<sup>rd</sup> bearing measured at shutdown and run-up before overhaul (see Fig. 4), 2009

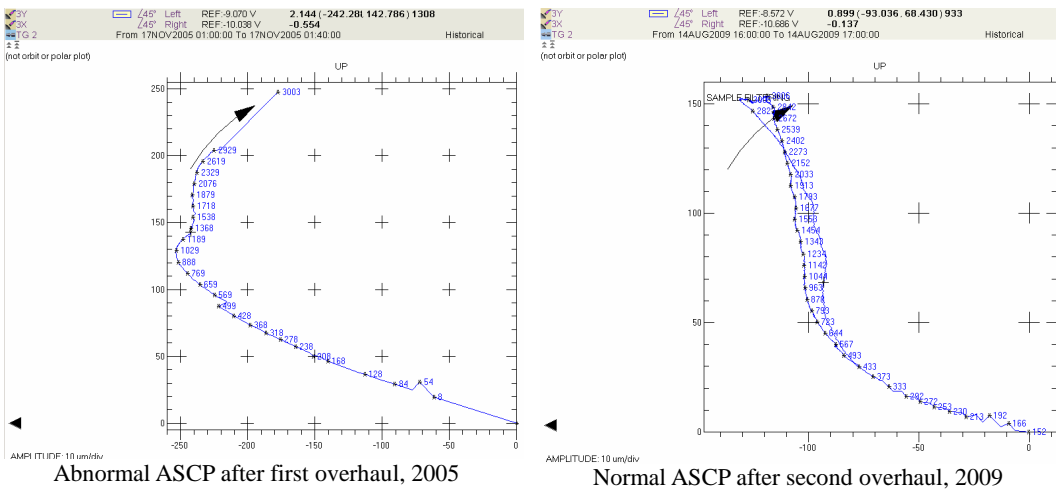


Fig. 6. ASCP with the new 3<sup>rd</sup> bearing after overhauls in 2005 and 2009

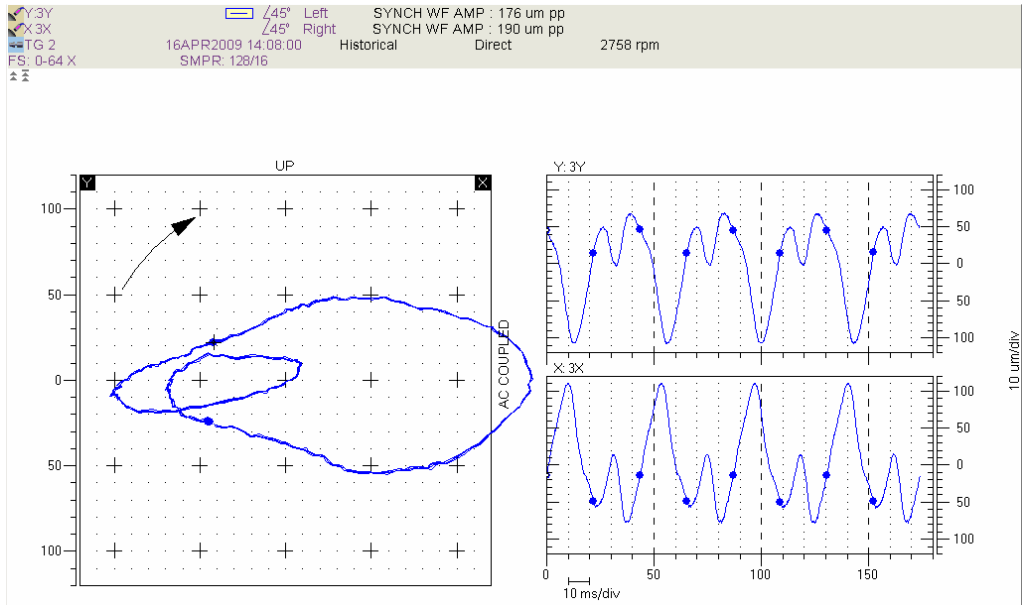


Fig. 7. The damaged 3<sup>rd</sup> bearing rotor orbit/time base plot at 2758 rpm during shut down

**Shaft kinetic orbit** In diagnostics practice it is difficult to verify that vibration frequency  $1/2X$  is an exact integer ratio by using only vibration signal spectrum, because of the limited resolution of the spectrum. To avoid such uncertainty a direct orbit with keyphasor dot display should be used to verify the integer relationship, Fig. 7. Because of its ease of interpretation and extensive information content, the orbit, with Keyphasor mark, is probably the most powerful single plot format available to the machinery diagnostician [1]. The Keyphasor mark on the orbit indicates the direction of increasing time, the direction of precession – from blank to dot sequence. If the frequency is constant, then the Keyphasor dots on direct orbits will remain locked in place through subsequent vibration cycle. If the keyphasor dots move along the path of the orbit, then the frequency is not an integer ratio. The two stationary sets of locked keyphasor dots on the direct orbit indicate exact  $1/2X=22.98$  Hz frequency self-excited vibration when rotor running speed is 2758 rpm ( $1X=45,97$  Hz), Fig. 7. The rubs as indicated in Fig. 4 result in very high vibration displacements, e. g.  $S_{y(p-p)\max}=176 \mu\text{m}$  and  $S_{x(p-p)\max}=190 \mu\text{m}$ ,  $S_{(p-p)\max}\approx 260 \mu\text{m}$  at 2758 rpm, Fig. 7. This complicated shape orbit demonstrates the path of the shaft centerline for eight shaft revolutions.

Fluid-steam induced instability produces subsynchronous vibration that is sometimes misdiagnosed as a rub, but fluid-steam induced instability produces self-excited vibration at a non-integer ratio (such as  $0,475X, \dots$ ) of frequencies. Orbit breathes in fluid (steam) induced instability [1].

### Modeling and simulation of journal bearing

Modeling and simulation of damaged journal bearing was provided including two rotors DSR and VSR supported by oil-film bearings and coupling. These general assumptions were made: the material of the rotors and coupling is elastic; shear forces are evaluated; the deflection of the rotor is produced by the displacement of points of the center line; the axial motion of the rotors is neglected; the semi couplings are treated as rigid. Finite element method (FEM) formulation has been chosen to study the dynamic and hydrodynamic processes of the



rotating system. The rotor dynamics is simulated by FEM when finite element consists of two nodes and five degrees of freedom (DOF) at each node (Fig. 8 a). The first and second DOF are displacements along y and z axes and the last three DOF are angles about X, Y and Z axes. Journal bearing hydrodynamics is simulated by FEM when the isoparametric nine-node finite elements are used (Fig. 8 b).

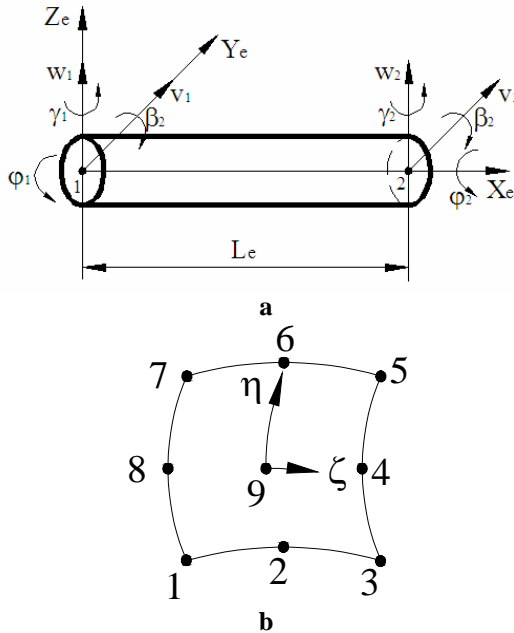


Fig. 8. Finite elements: a – rotor FEM; b – journal bearing FEM

**Solution of dynamic equilibrium equations**

The system of equations of motion of the rotating system can be written in the form:

$$[M(q)]\{\ddot{q}\} + ([C] + [G(\dot{q})])\{\dot{q}\} + [K(q)]\{q\} = \{F(q, \dot{q}, t)\}. \quad (1)$$

**Solution of hydrodynamics equations** Oil pressure distribution is obtained by Reynolds equation [8]

$$\frac{\partial}{\partial x} \left( \frac{h^3}{\mu} k_x \frac{\partial p}{\partial x} \right) + \frac{\partial}{\partial s} \left( \frac{h^3}{\mu} k_s \frac{\partial p}{\partial s} \right) = \frac{\partial h}{\partial t} + \frac{\partial}{\partial x} (hU_x) + \frac{\partial}{\partial s} (hU_s) \quad , \quad (2)$$

where  $s$  is circumferential coordinate,  $s = R_B \theta$  (Fig. 9);  $x$  lies on the surface and is parallel to longitudinal axis of journal bearing;  $h(x, s, t)$  is the lubricating film thickness;  $U_x, U_s$  are velocity components in the  $x$  and  $s$  directions,  $U_s = \frac{1}{2} R_R (\dot{\phi}_R - 2\dot{\psi})$ ;  $k_x, k_s$  axial and circumferential turbulence coefficients in laminar dynamic:  $k_x = 1/12, k_s = 1/12$ ;

in turbulent dynamic:  $k_x = \frac{1}{12 + 0,0144R_e^{0,854}} ; k_s = \frac{1}{12 + 0,01392R_e^{0,9}} ;$  (3)

Reynolds number is equal  $Re = \rho U_s c / \mu$ .

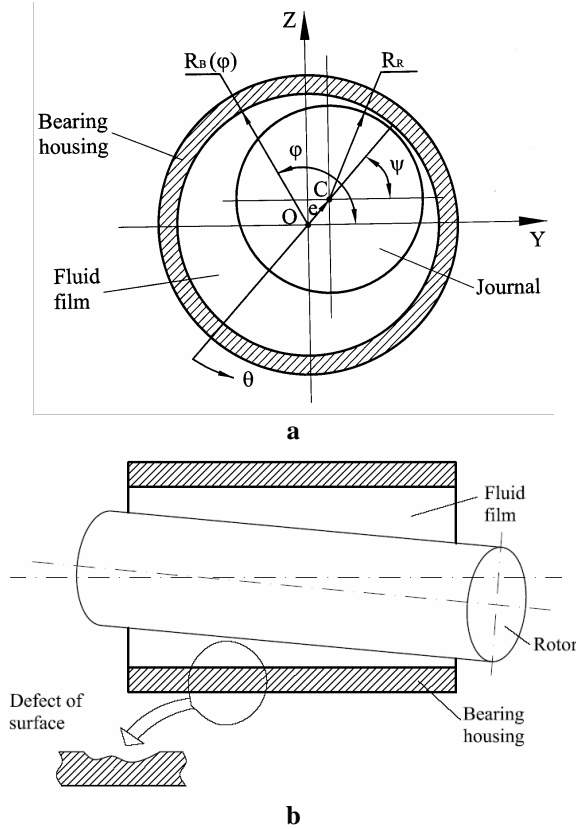


**Fig. 9.** Geometry of the journal bearing

The film thickness can be written in the form (Fig. 8)

$$h = R_B(\varphi_B) - R_R(\varphi_R) - v \cos(\psi) - w \sin(\psi), \quad (4)$$

where  $\psi = \arctan(w/v)$ .

The sliding surface of the bearing has defects as presented in Fig. 9 b and Fig. 10. The derivatives of the film thickness can be written:

$$\frac{\partial h}{\partial t} = -\dot{v} \cos(\psi) - \dot{w} \sin(\psi) - v \dot{\psi} \sin^2(\psi) - w \dot{\psi} \cos^2(\psi) + (v \dot{w} + w \dot{v}) \sin(\psi) \cos(\psi) \quad (5)$$

$$\frac{\partial h}{\partial x} = \frac{\partial h}{\partial v} \frac{\partial v}{\partial x} + \frac{\partial h}{\partial w} \frac{\partial w}{\partial x}, \quad (6)$$

$$\frac{\partial h}{\partial v} = -\frac{v}{e}; \quad \frac{\partial h}{\partial w} = -\frac{w}{e}; \quad e = \sqrt{v^2 + w^2};$$

$$\frac{\partial v}{\partial x} = \frac{\partial [N_v(\xi)]}{L_e \partial \xi} \{q_e\}; \quad \frac{\partial w}{\partial x} = \frac{\partial [N_w(\xi)]}{L_e \partial \xi} \{q_e\}.$$

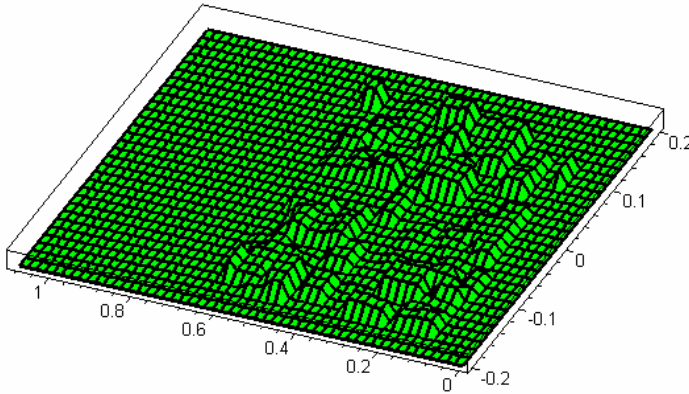


**Fig. 10.** Geometry of the sliding surface of the journal bearing

Oil pressure distribution in the journal bearing is obtained from total system of equations

$$[H(q)]\{P\} = \{B(q, \dot{q})\}, \quad (7)$$

with boundary conditions

$$P(x=0, s) = p_a, \quad P(x=b, s) = p_a,$$

$$P(x, s=0) = p_a, \quad P(x, s=2 * \pi R_B) = p_a, \quad (8)$$

In an implicit time integration scheme, equilibrium of the system (1) is considered to obtain the solution at time  $t + \Delta t$ . The nonlinear system is solved using the Newton-Raphson method. The system of equations (1) and (7) are solved by using iteration process.

The selection of an appropriate time step  $\Delta t$  is very important to the accuracy of simulation and analysis. Since the time integration scheme employed is implicit, its stability is unaffected by the size of the time step. In an implicit, unconditionally stable time integration scheme  $\Delta t$  should be small enough that the response in all modes which significantly contribute to the total structural response is calculated with high accuracy. The time step of  $10^{-5}$  s was selected for use in the integration process.

Two steel rotors with coupling rotating at 3000 rpm and supported at the four journal bearings are considered. The defects are characterized by the volume. The volume of defects is equal to:

$$V_{def} = \sum_{k=1-1-1-1}^{NE} \int \int \int \det([J_k]) d\zeta d\eta d\varsigma = 0,378 \cdot 10^{-9} \text{ m}^3.$$

The sliding surface of VSR 3<sup>rd</sup> journal bearing with geometry defects is illustrated in Fig. 11.

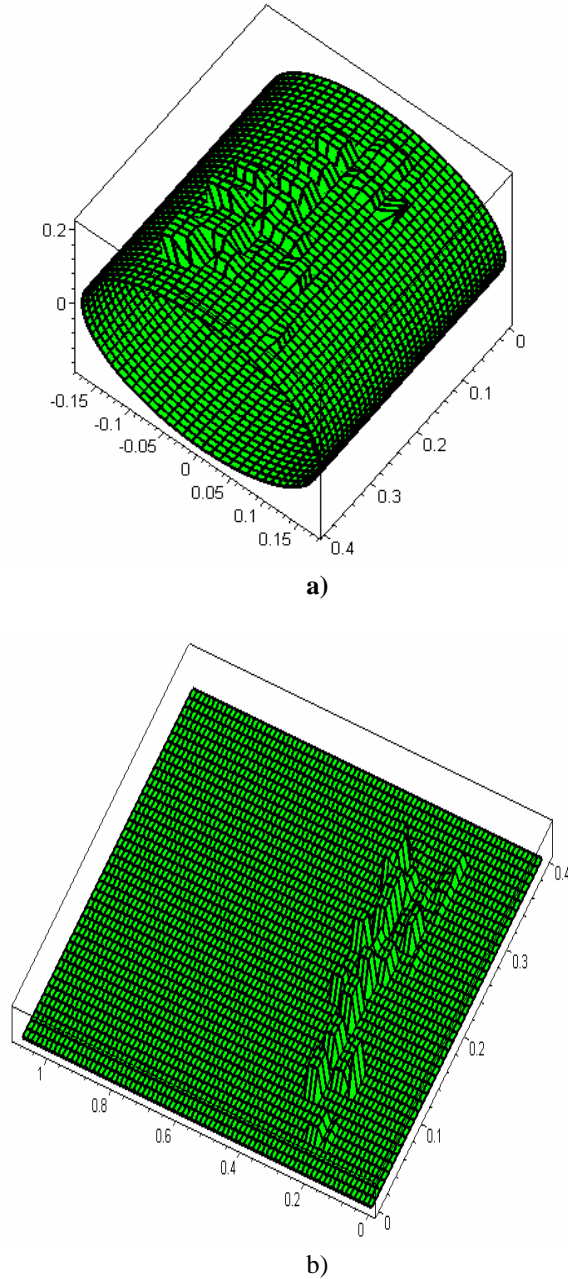


**Fig. 11.** The 3<sup>rd</sup> journal bearing surface with geometry defects: a – sliding cylinder; b – evolvent of cylinder

Simulated pressure (vertical axis) distribution on the 3<sup>rd</sup> journal bearing surface in the different time are given in Fig. 12.

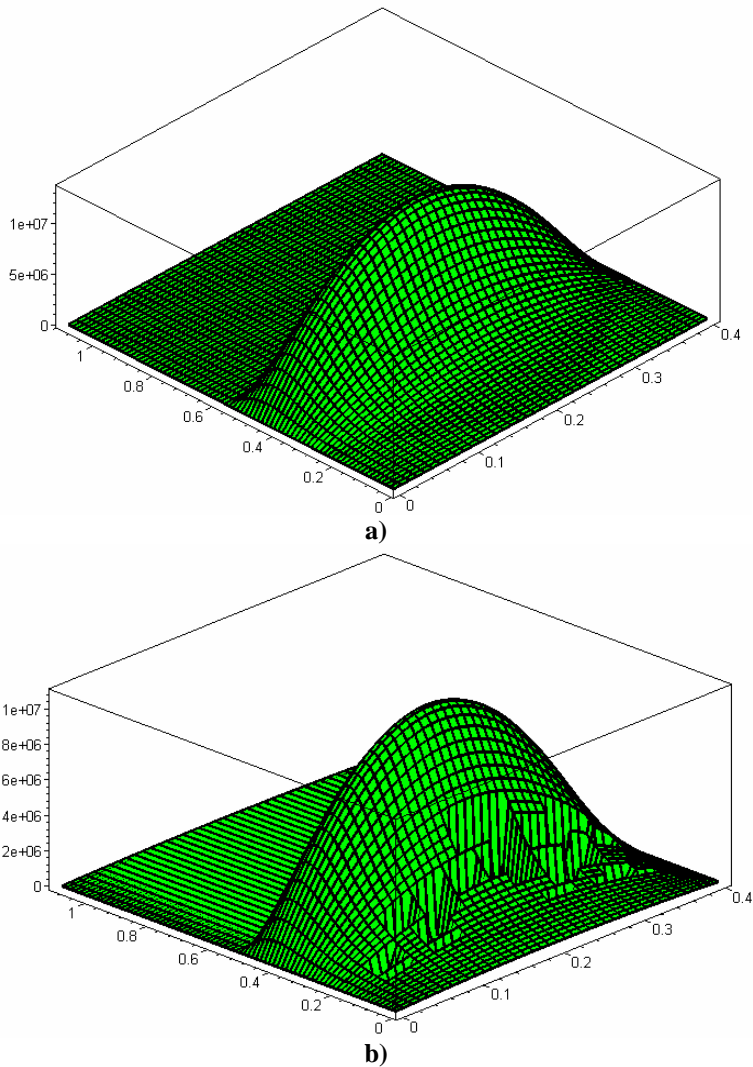


**Fig. 12.** Pressure (Pa) distribution on the 3<sup>rd</sup> journal bearing surface:  
a -  $\psi = 0$  degrees; b -  $\psi = 200$  degrees

## Conclusions

Some conclusions can be formulated on the basis of the reported research work:  
1. The partial radial rub in the 3<sup>rd</sup> bearing led to damaged upper part Babbitt metal of the bearing. The rubs occurred at rotational speeds of rotors: at run-up started at ~2758 rpm, which is twice as large as the first balance resonance speed ~1379 rpm of turbounit rotating system (1/2X subharmonics frequency). The rubbing continues up to 2900 rpm at run-up, reoccurs at the shutdown mode and continues during ~150 rpm rotational speed interval.

2. The rubbing in the 3<sup>rd</sup> bearing was induced by large initial vertical misalignment of two rotors (DSR and VSR) when connected with coupling during the first overhaul. Radial gap between shaft and bearing was reduced in upper part of the bearing and during all period of operation the 3<sup>rd</sup> bearing was only partially loaded.
3. For old design long-time-used machines after renovation and installation of MDS with sensors for measurement of rotors relative vibration displacements (without seismic transducer measuring absolute vibration parameters) the rubbing diagnostics is effective with the main data formats: vibration displacement direct and synchronous 1X trend plots, ASCP, direct orbit and full spectrum plots.
4. Simulations with the developed rotating system numerical model enabled evaluation of the extent of damage on the journal bearing.

### Acknowledgement

Research was supported by the Lithuanian State Science Foundation and JSC “Kaunas Thermo Power Plant” Lithuania, Grants Nr. 8464, 8526.

### References

- [1] **Bently D. E., Charles T. H.** *Fundamentals of Rotating Machinery Diagnostics*, (2002) pp.726, Printed in Canada, first printing.
- [2] **Muszynska Agnieszka (Agnes).** *Rotordynamics*, (2005) pp.1075, CRC Press Taylor and Francis Group.
- [3] **Bently D. E.** Rotating Machinery Measurements 101. *Orbit*, Vol. **15**, No.2(1994), pp.4-6, Bently Nevada, Minden, USA.
- [4] **Mažeika P.** Diagnostics and Failures prevention Researches of Rotors with Rolling Element Bearings. *Summary of Doctoral Dissertation*, 2008, pp.36, Kaunas University of Technology Press. Technologija, Lithuania, UDK 62-251 (043).
- [5] **Goldin A. S.** *Vibration of Rotating Machines*, (2000) pp.344. – Moscow: Mashinostroenie, (in Russian).
- [6] **Barzdaitis V., Jonušas R., Didžiokas R., Barzdaitis V. V.** Absolute and Relative Vibration Inconsistencies in Dynamic Analysis of High Power Turbogenerator Rotating System. *Proc.3<sup>rd</sup> International Congress of Technical Diagnostics*, Vol.**30**, tom**1**, pp.45-52. Poznan, Poland, September (2004).
- [7] **Bachschnid N., Pennacchi P., Chartterton S., Ricci R.** On Model Updating of Turbo-Generator Sets, *JVE journal of Vibroengineering*, Vol. **11**, Issue **3** (2009), pp.379-391, Vibromechanika, Vilnius, Lithuania.
- [8] **Aladjev V., Bogdevičius M.** Maple: *Programing, Physical and Engineering Problems*, (2006) pp.404 Fultus Books, USA.